Electronic Supplementary Material (ESI) for CrystEngComm.

Supplementary Information

Polymorphism of the ternary complex (2-amino-5-chloropyridine)·(9-anthracenecarboxylic acid)·(trinitrobenzene)

Atiyyah Salajee

A. Molecular Overlay

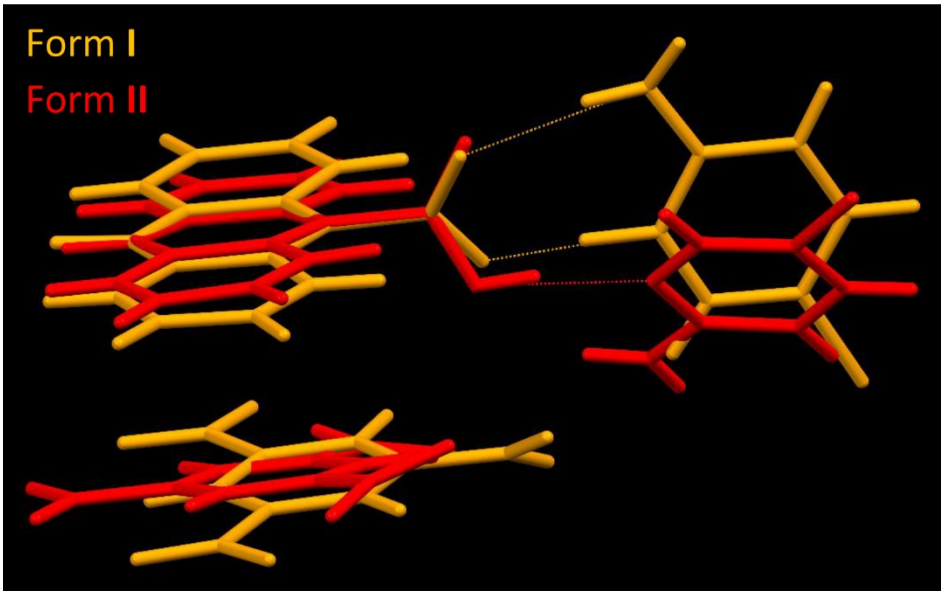

Figure S1. Overlays of pairs of polymorphs showing the relative positions to the common 9-aca molecule.

B. Difference Fourier Maps

Difference Fourier maps for forms **I** and **II** were generated using PLATON, to identify the location of the proton in order to determine whether proton transfer occurred between O7 and N4.

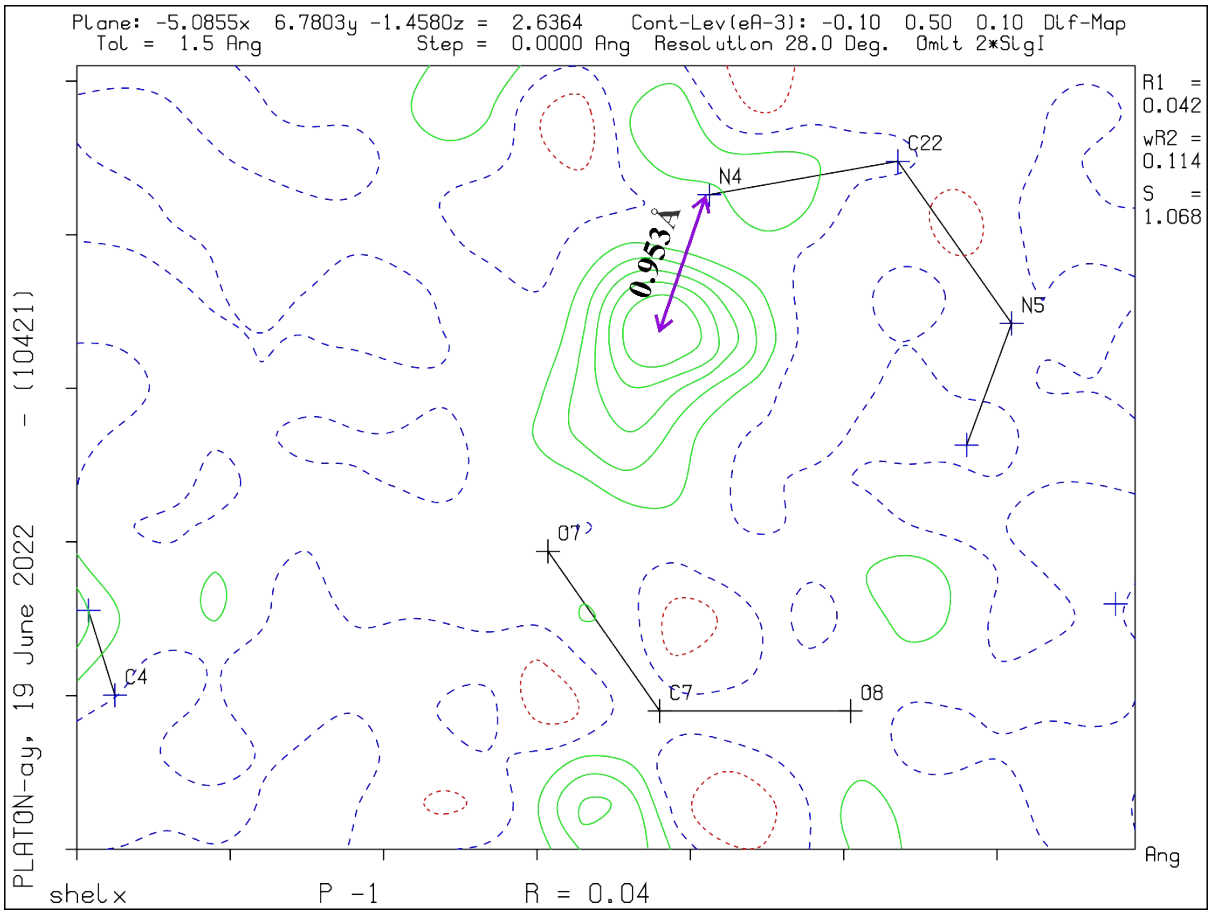

Figure S2. Difference Fourier map of form **I**.

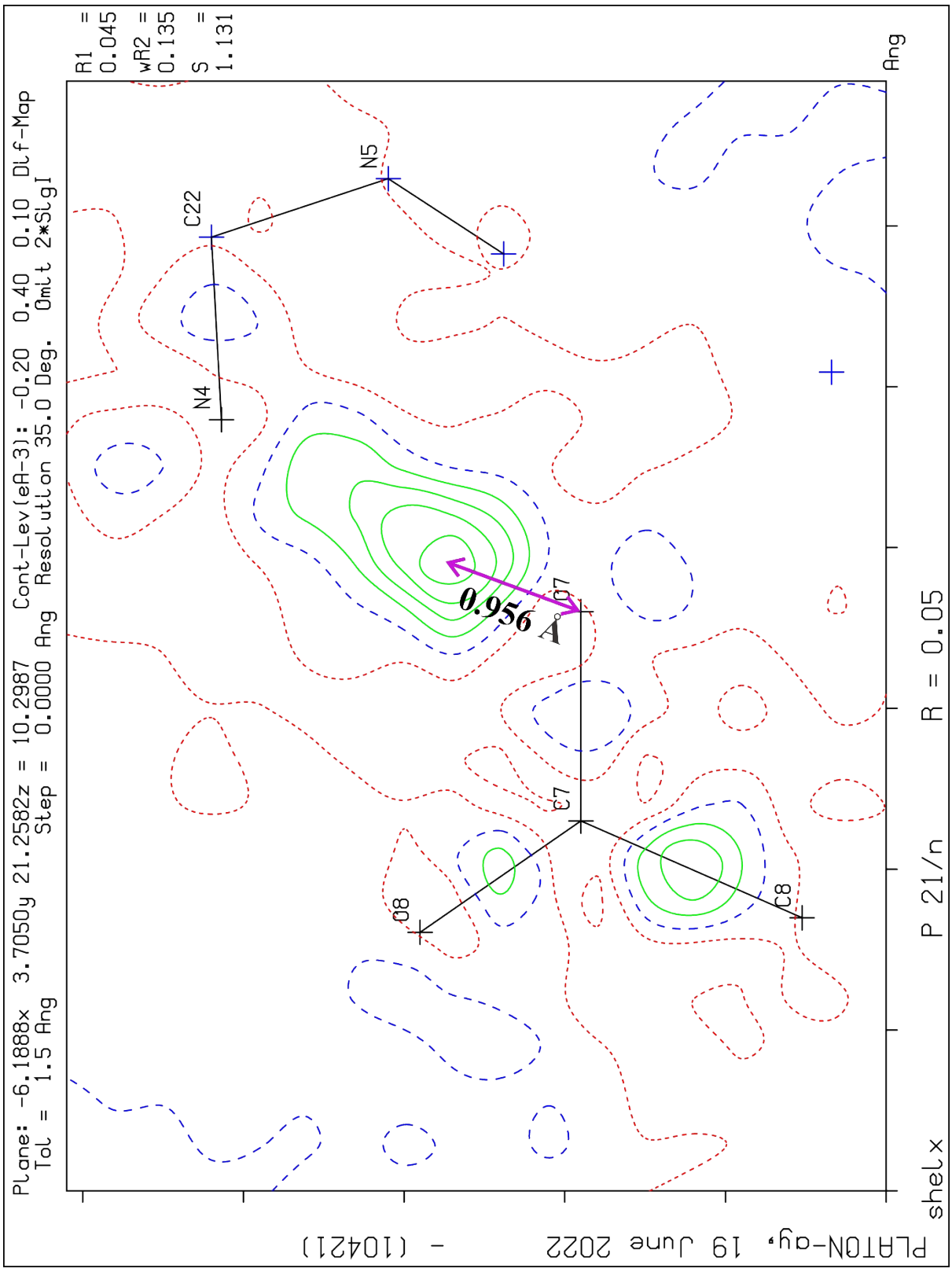

Figure S3. Difference Fourier map of form **II**.

C. Intermolecular Potentials

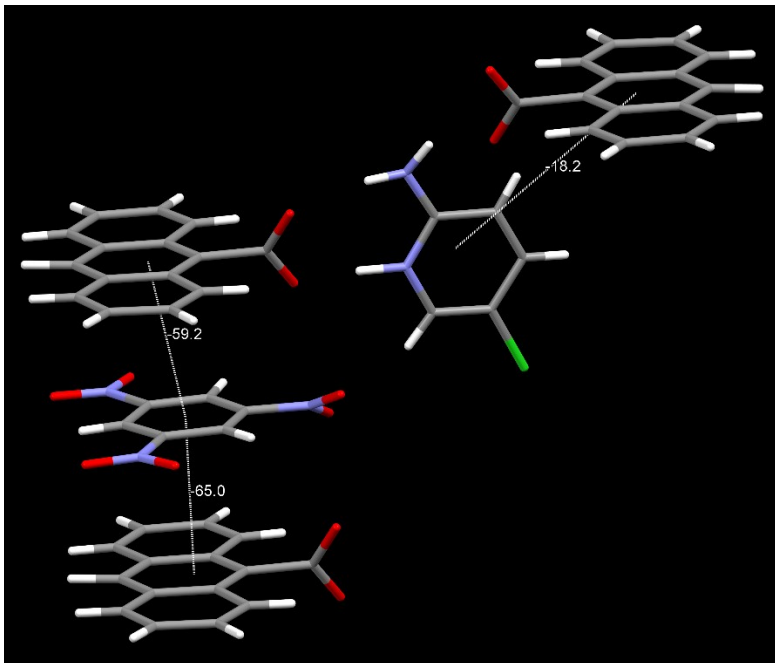

Figure S4. Calculated intermolecular potentials using the UNI force field for Form **I**. Only the strongest three are shown.

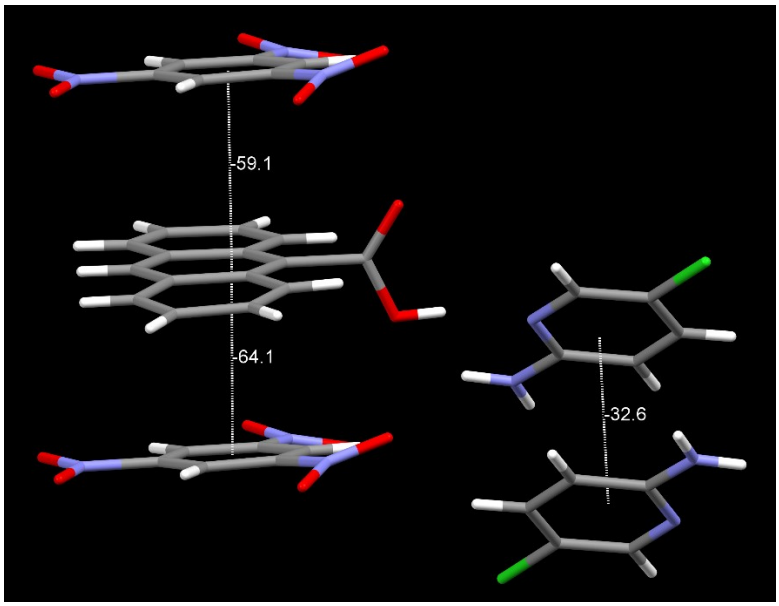

Figure S5. Calculated intermolecular potentials using the UNI force field for Form **II**. Only the strongest three are shown.

D. Experimental Setup

All reagents used for synthesis and characterization were of analytical grade, purchased from Sigma-Aldrich, unless otherwise stated. Reagents were used as received, without further purification. In most experiments, a 1:1:1 stoichiometric ratio was used. 20 mg of trinitrobenzene (0.094 mmol), 20 mg of 9-anthracenecarboxylic acid (0.090 mmol) and 12 mg of 2-amino-5-chloropyridine (0.093 mmol) were weighed out. In some experiments, the amount of pyridine used was increased, giving stoichiometric ratios of 1:1:2 and 1:1:3 of tnb:9aca:2a5clp. All solutions were heated and stirred.

Table S1. Crash Crystallization Experiments*

Solvent	Result
ethanol (1mL)	Form **I**
ethanol (2mL)	Form **I** and **II**
methanol (1mL)	Form **I** and **II**
methanol (2mL)	Form **I** and **II**
isopropanol (1mL)	Form **I** and **II**
isopropanol (2mL)	Form **I** and **II**

*orange seed crystals were added to promote the formation of form **I**.

Table S2. Slow Evaporation Experiments

Solvent System		Temperature	Stoichiometric Ratio	Result
acetonitrile		room temperature	1:1:1	Form **I**
		room temperature	1:1:2	Form **I**
		room temperature	1:1:3	Form **I**
		oven @ 36°C	1:1:1	Form **I** and **II**
ethanol		room temperature	1:1:1	Form **I** and **II**
		room temperature	1:1:3	Form **I**
		oven @ 36°C	1:1:3	Form **I** and **II**
methanol		room temperature	1:1:1	Form **II**
		oven @ 36°C	1:1:1	Form **I** and **II**
acetonitrile/ethanol	1:1	room temperature	1:1:1	Form **I** and **II**
	2:1	room temperature	1:1:1	Form **I** and **II**
	3:1	room temperature	1:1:1	Form **I** and **II**
	1:2	room temperature	1:1:1	Form **I** and **II**
	1:3	room temperature	1:1:1	Form **I** and **II**
	1:1	oven @ 36°C	1:1:1	Form **II**
	2:1	oven @ 36°C	1:1:1	Form **II**
	3:1	oven @ 36°C	1:1:1	Form **II**
	1:2	oven @ 36°C	1:1:1	Form **II**
	1:3	oven @ 36°C	1:1:1	Form **II**
ethyl acetate/toluene	1:1	room temperature	1:1:1	Form **II**
	2:1	room temperature	1:1:1	Form **II**
	3:2	room temperature	1:1:1	Form **II**
	1:1	oven @ 36°C	1:1:1	Form **I**
	3:1	oven @ 36°C	1:1:1	Form **I**
	3:2	oven @ 36°C	1:1:1	Form **II**

Slurry experiments:

1. Stoichiometric amounts of **tnb**, **9aca**, and **2a5clp** were combined in a sample vial. Hexane was the solvent of choice since the starting reagents were insoluble in it. The vial was sealed, and the mixture was left to stir for 24hrs. Thereafter, the vial was opened to allow the remaining hexane to evaporate. A red powder remained.
2. Red and orange crystals (5mg each), of forms **I** and **II** respectively, were placed in a vial with hexane. The vial was sealed, and the mixture left to stir for 24hrs. Thereafter, the vial was opened to allow the remaining hexane to evaporate. A red powder formed.

E. Single Crystal Diffraction Data

All data collections were obtained on a Bruker Venture D8 Photon CMOS diffractometer with graphite-monochromated MoKα_1 (λ = 0.71073 Å) radiation at 173 K using an Oxford Cryostream Plus cooler. The collection method involved ω-scans with a 0.5° width. SAINT+ version 6.02.6[1] software was used for data reduction and *SADABS*[2] was used to make empirical absorption corrections. The crystal structures were solved using direct methods on *SHELXS-97*.[3] Non-hydrogen atoms were first refined isotropically, followed by anisotropic refinement by full matrix least-squares calculations based on F^2 using *SHELXL-2017*.[3] C-bound H atoms were located in the difference map, then positioned geometrically and were allowed to ride on their respective parent atoms, with thermal displacement parameters 1.2 times of the parent C atom. For Form **I** and **II,** the coordinates and isotropic displacement parameters of the N-bound amine H atoms involved in hydrogen bonding interactions were allowed to refine freely. For Form **I**, the N-bound pyridine H atom was placed geometrically and was allowed to ride on its respective parent atom, with thermal displacement parameters 1.2 times of the parent N atom. For Form **II**, the O-bound H atom was placed geometrically and was allowed to ride on its respective parent atom, with thermal displacement parameters 1.5 times of the parent O atom. For the positional disorder model appled to form I and II, the same procedure was used. The N-bound pyridine H atom and O-bound carboxylic acid H atom were placed geometrically (both ride on their parent atoms and have their thermal displacement parameters 1.2 times of the parent N atom or 1.5 times of the parent O atom) and their relative site-occupancies refined freely. For form **I**, this gave a ratio of 0.69(3) (N-bound H) to 0.31(3) (O-bound) and for form **II**, 0.69(3) (O-bound H) to 0.31(3) (N-bound). Diagrams and publication material were generated using *WinGX*,[4] *ORTEP-3*,[4] *PLATON*[5] and *MERCURY*.[6]

1. SAINT+, Version 6.02 (Includes XPREP and SADABS); Bruker AXS Inc: Madison, Wisconsin, USA, 2004.
2. Krause, L., Herbst-Irmer, R., Sheldrick, G. M. & Stalke, D. (2015). J. Appl. Cryst. 48, 3–10.
3. Sheldrick, G. M., Acta Crystallogr., Sect. C. 2015, 71 (Pt 1), 3-8.
4. Farrugia, L., J. Appl. Crystallogr. 2012, 45 (4), 849-854.
5. Spek, A., Acta Crystallogr., Sect. D. 2009, 65 (2), 148-155.
6. C. F. Macrae, I. Sovago, S. J. Cottrell, P. T. A. Galek, P. McCabe, E. Pidcock, M. Platings, G. P. Shields, J. S. Stevens, M. Towler and P. A. Wood, J. Appl. Cryst. 2020, 53, 226-235.

Table S3. Crystal data and structure refinement for **Form I**

Identification code	Form **I**	
Empirical formula	C26 H18 Cl N5 O8	
Formula weight	563.90	
Temperature	173(2) K	
Wavelength	0.71073 Å	
Crystal system	Triclinic	
Space group	P -1	
Unit cell dimensions	a = 7.1140(2) Å	α= 88.738(2)°.
	b = 9.7490(3) Å	β= 81.565(2)°.
	c = 18.0972(5) Å	γ = 89.703(2)°.
Volume	1241.24(6) $Å^3$	
Z	2	
Density (calculated)	1.509 Mg/m^3	
Absorption coefficient	0.217 mm^{-1}	
F(000)	580	
Crystal size	0.495 x 0.150 x 0.098 mm^3	
Theta range for data collection	2.089 to 27.992°.	
Index ranges	-9<=h<=9, -12<=k<=12, -23<=l<=23	
Reflections collected	47374	
Independent reflections	5991 [R(int) = 0.0390]	
Completeness to theta = 25.242°	100.0 %	
Absorption correction	Semi-empirical from equivalents	
Max. and min. transmission	0.7457 and 0.7108	
Refinement method	Full-matrix least-squares on F^2	
Data / restraints / parameters	5991 / 0 / 367	
Goodness-of-fit on F^2	1.062	
Final R indices [I>2sigma(I)]	R1 = 0.0406, wR2 = 0.1006	
R indices (all data)	R1 = 0.0612, wR2 = 0.1109	
Extinction coefficient	n/a	
Largest diff. peak and hole	0.290 and -0.427 $e.Å^{-3}$	
CCDC identification code	2157390	

Table S4. Hydrogen bonds for Form **I** [Å and °].

D-H···A	d(D-H)	d(H···A)	d(D···A)	<(DHA)
N5-H5B···O8(i)	0.90(2)	2.23(2)	2.9687(19)	138(2)
N4-H4A···O7	0.88	1.70	2.5762(16)	171(2)

Symmetry transformations used to generate equivalent atoms:

(i) -x,-y+1,-z+1

Table S5. Crystal data and structure refinement for **Form II**

Identification code	Form **II**	
Empirical formula	C26 H18 Cl N5 O8	
Formula weight	563.90	
Temperature	153(2) K	
Wavelength	0.71073 Å	
Crystal system	Monoclinic	
Space group	P 21/n	
Unit cell dimensions	a = 8.9341(5) Å	α= 90°.
	b = 7.2129(4) Å	β= 94.311(2)°.
	c = 38.172(2) Å	γ = 90°.
Volume	2452.8(2) $Å^3$	
Z	4	
Density (calculated)	1.527 Mg/m^3	
Absorption coefficient	0.220 mm^{-1}	
F(000)	1160	
Crystal size	0.404 x 0.291 x 0.276 mm^3	
Theta range for data collection	2.874 to 27.999°.	
Index ranges	-11<=h<=11, -9<=k<=9, -50<=l<=50	
Reflections collected	71399	
Independent reflections	5853 [R(int) = 0.0140]	
Completeness to theta = 25.242°	98.4 %	
Refinement method	Full-matrix least-squares on F^2	
Data / restraints / parameters	5853 / 0 / 370	
Goodness-of-fit on F^2	1.062	
Final R indices [I>2sigma(I)]	R1 = 0.0375, wR2 = 0.0997	
R indices (all data)	R1 = 0.0381, wR2 = 0.1001	
Extinction coefficient	n/a	
Largest diff. peak and hole	0.371 and -0.303 $e.Å^{-3}$	
CCDC identification code	2157391	

Table S6. Hydrogen bonds for form **II** [Å and °].

D-H···A	d(D-H)	d(H···A)	d(D···A)	<(DHA)
N5-H5A···O4(i)	0.88(2)	2.42(2)	3.1834(16)	145(2)
N5-H5B···O4(ii)	0.85(2)	2.29(2)	3.1065(15)	162(2)
O7-H7···N4	0.84	1.71	2.5392(12)	167

Symmetry transformations used to generate equivalent atoms:

(i) x,y+1,z (ii) -x+2,-y+1,-z+1

Table S7. Crystal data and structure refinement for **Form I disorder**

Identification code	Form **I** disorder	
Empirical formula	C26 H18 Cl N5 O8	
Formula weight	563.90	
Temperature	173(2) K	
Wavelength	0.71073 Å	
Crystal system	Triclinic	
Space group	P -1	
Unit cell dimensions	a = 7.1140(2) Å	α= 88.738(2)°.
	b = 9.7490(3) Å	β= 81.565(2)°.
	c = 18.0972(5) Å	γ = 89.703(2)°.
Volume	1241.24(6) $Å^3$	
Z	2	
Density (calculated)	1.509 Mg/m^3	
Absorption coefficient	0.217 mm^{-1}	
F(000)	580	
Crystal size	0.495 x 0.150 x 0.098 mm^3	
Theta range for data collection	2.089 to 27.992°.	
Index ranges	-9<=h<=9, -12<=k<=12, -23<=l<=23	
Reflections collected	47374	
Independent reflections	5991 [R(int) = 0.0390]	
Completeness to theta = 25.242°	100.0 %	
Absorption correction	Semi-empirical from equivalents	
Max. and min. transmission	0.7457 and 0.7108	
Refinement method	Full-matrix least-squares on F^2	
Data / restraints / parameters	5991 / 0 / 371	
Goodness-of-fit on F^2	1.061	
Final R indices [I>2sigma(I)]	R1 = 0.0403, wR2 = 0.0988	
R indices (all data)	R1 = 0.0609, wR2 = 0.1091	
Extinction coefficient	n/a	
Largest diff. peak and hole	0.292 and -0.425 $e.Å^{-3}$	
CCDC identification code	2181218	

Table S8. Hydrogen bonds for Form **I** disorder [Å and °].

D-H···A	d(D-H)	d(H···A)	d(D···A)	<(DHA)
N5-H5B···O8(i)	0.90(2)	2.24(2)	2.9687(19)	138(2)
N4-H4A···O7	0.88	1.70	2.5762(16)	171
O7-H7···N4	0.84	1.76	2.5762(16)	162

Symmetry transformations used to generate equivalent atoms:

(i) -x,-y+1,-z+1

Table S9. Crystal data and structure refinement for **Form II disorder**

Identification code	Form **II** disorder	
Empirical formula	C26 H18 Cl N5 O8	
Formula weight	563.90	
Temperature	153(2) K	
Wavelength	0.71073 Å	
Crystal system	Monoclinic	
Space group	P 21/n	
Unit cell dimensions	a = 8.9341(5) Å	α= 90°.
	b = 7.2129(4) Å	β= 94.311(2)°.
	c = 38.172(2) Å	γ = 90°.
Volume	2452.8(2) $Å^3$	
Z	4	
Density (calculated)	1.527 Mg/m^3	
Absorption coefficient	0.220 mm^{-1}	
F(000)	1160	
Crystal size	0.404 x 0.291 x 0.276 mm^3	
Theta range for data collection	2.874 to 27.999°.	
Index ranges	-11<=h<=11, -9<=k<=9, -50<=l<=50	
Reflections collected	71383	
Independent reflections	5853 [R(int) = 0.0140]	
Completeness to theta = 25.242°	98.4 %	
Absorption correction	Semi-empirical from equivalents	
Max. and min. transmission	0.7471 and 0.7007	
Refinement method	Full-matrix least-squares on F^2	
Data / restraints / parameters	5853 / 0 / 371	
Goodness-of-fit on F^2	1.076	
Final R indices [I>2sigma(I)]	R1 = 0.0372, wR2 = 0.0987	
R indices (all data)	R1 = 0.0377, wR2 = 0.0991	
Extinction coefficient	n/a	
Largest diff. peak and hole	0.368 and -0.298 $e.Å^{-3}$	
CCDC identification code	2181219	

Table S10. Hydrogen bonds for form **II** disorder [Å and °].

D-H···A	d(D-H)	d(H···A)	d(D···A)	<(DHA)
N5-H5A···O4(i)	0.89(2)	2.42(2)	3.1831(16)	145(2)
N5-H5B···O4(ii)	0.84(2)	2.30(2)	3.1065(15)	162(2)
N4-H4A···O7	0.88	1.66	2.5390(12)	172
O7-H7···N4	0.84	1.71	2.5390(12)	167

Symmetry transformations used to generate equivalent atoms:

(i) x,y+1,z (ii) -x+2,-y+1,-z+1

F. Fourier Transform Infrared Spectroscopy

FTIR spectra of the samples were collected using a Bruker Alpha II, fitted with an ATR eco ZnSe crystal, with a spectral range of 20 000 – 500 cm^{-1}. OPUS software, *version* 8.5, was used to analyse and characterize the spectra.

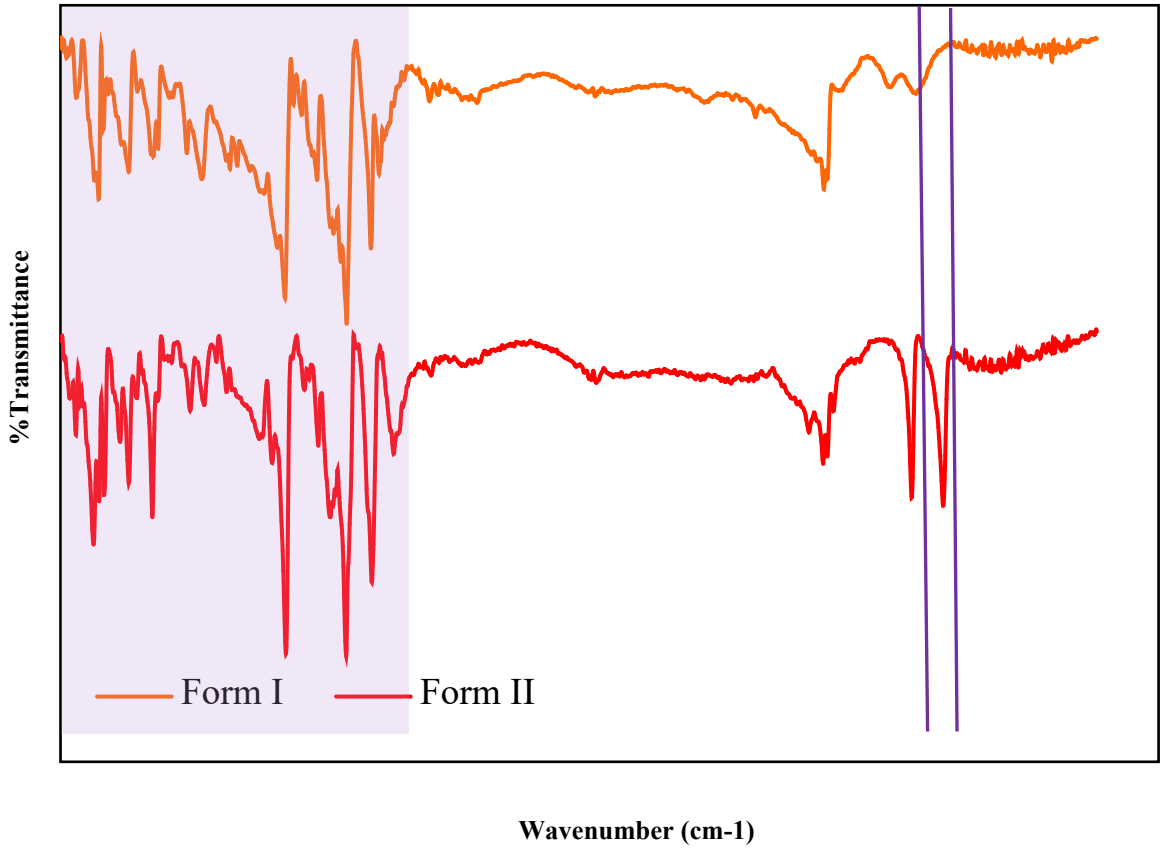

Figure S6. Infrared spectra of Forms **I** and **II**. The shaded region and the two peaks indicated by the solid purple lines are convenient for distinguishing the two forms.

Table S11. Infrared Spectral Analysis.

Assignment	Functional group	Wavenumber (cm^{-1}) Form **I**	Wavenumber (cm^{-1}) Form **II**
N – H stretch	Primary amine (produces 2 bands)	3405, 3316 (w, br)	3493, 3390 (m, sharp)
N – H bend	Primary amine	1617 (m)	1620 (s)
C = O stretch	Carboxylic acid	-	1692 (m, sharp)
C – O stretch	Carboxylic acid	-	1339 (s, sharp)
CO_2^- asymmetric stretch	Carboxylate	1644 (w, br)	-
CO_2^- symmetric stretch	Carboxylate	1335 (m, br)	-
O – H stretch	Carboxylic acid	absent	3200-2900 (broad, s)
N – H stretch	Pyridinium salt	3102 (broad, s)	absent
N – O stretch	Nitro compound	1537 (s)	1537 (s)

The most striking difference between the IR spectra of form **I** and form **II** are the two N – H stretching peaks of the amino group. In form **I**, the two N – H stretches are broad and weak, and their position is shifted to a lower wavenumber as compared to that of form **II**. In contrast, the two N – H stretches in form **II** are significantly stronger and narrower, and at a higher wavenumber than that of form **I**. The next difference is less apparent and can be associated with the subsequent peak in both spectra. In the spectrum of form **II**, the broad peak ranging from 3200-2900 cm^{-1}, can be assigned as the O – H stretch of the carboxylic acid in 9aca. The small narrow bumps on this broad O – H peak can be attributed to aromatic C – H stretching peaks, which fall in the same wavenumber range as the O – H stretches. In form **I**, the broad yet sharp peak at around 3100 cm^{-1} can be assigned to the N – H stretch of the protonated pyridine of the $2a5clp^{(+)}$ cation. This provides evidence that form **I** is a salt, since it lacks the O – H carboxylic acid stretch and instead contains an N – H pyridinium salt stretch which is indicative of proton transfer. Furthermore, it proves that form **II** is a cocrystal since it contains the O – H carboxylic acid stretch, which indicates retention of the proton by the carboxylic acid.

G. Powder X-ray Diffraction

Powder X-ray diffraction data patterns were collected at 293 K on a Bruker D2 Phaser diffractometer which employed a sealed tube Co X-ray source (= 1.78897 Å), operating at 30 kV and 10 mA, and LynxEye PSD detector in Bragg-Brentano geometry. The calculated powder diffraction patterns were computed from the single crystal data which was collected at 173 K using Mercury. The peak positions are shifted resulting from the different temperatures at which the samples were measured. The peak intensities vary due to preferred orientation.

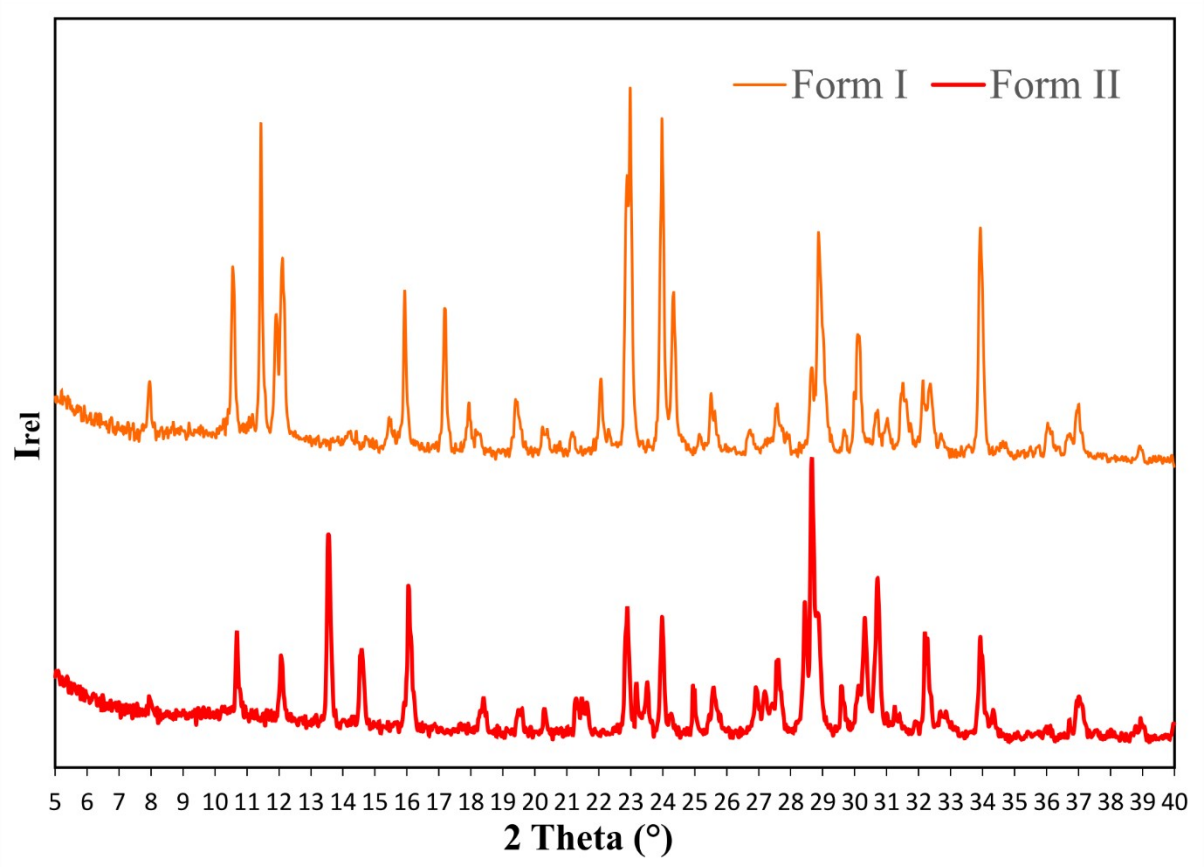

Figure S7. Measured PXRD of forms **I** and **II**.

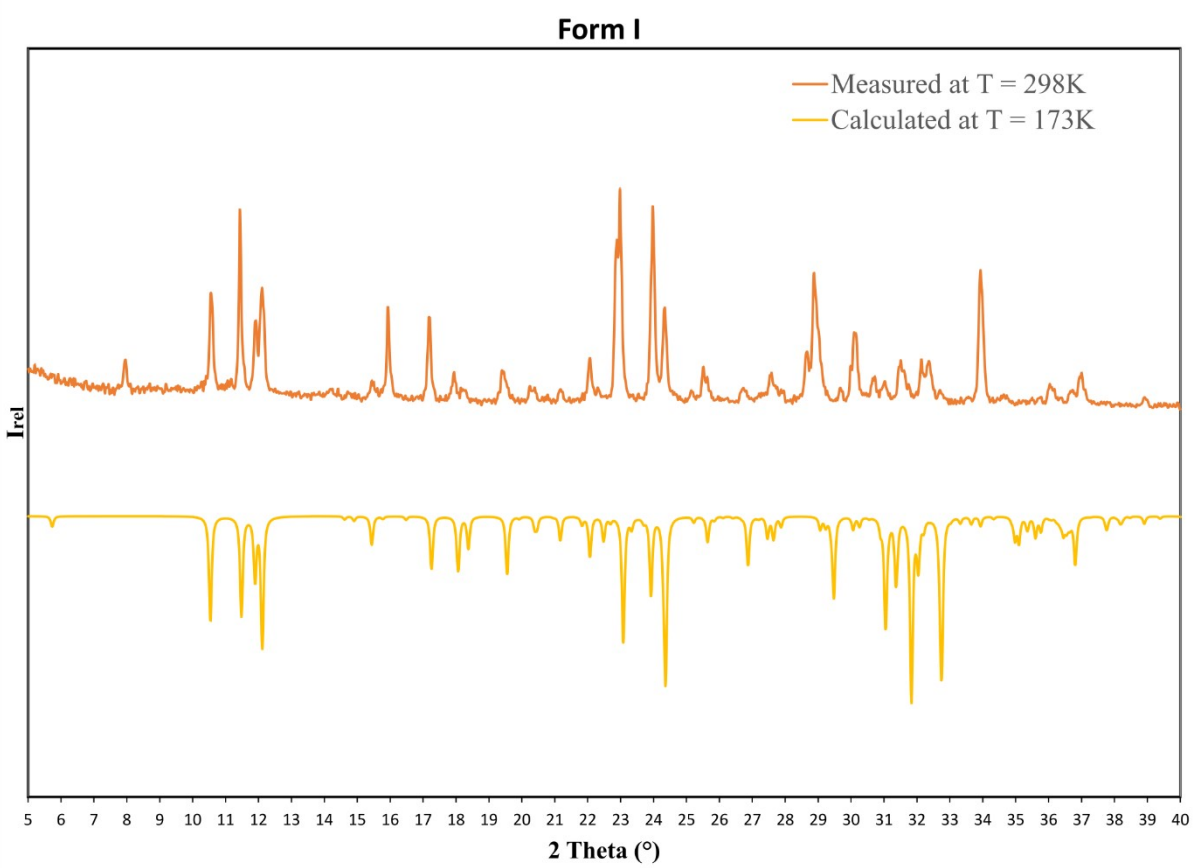

Figure S8. Measured vs. calculated PXRD of the orange form **I**

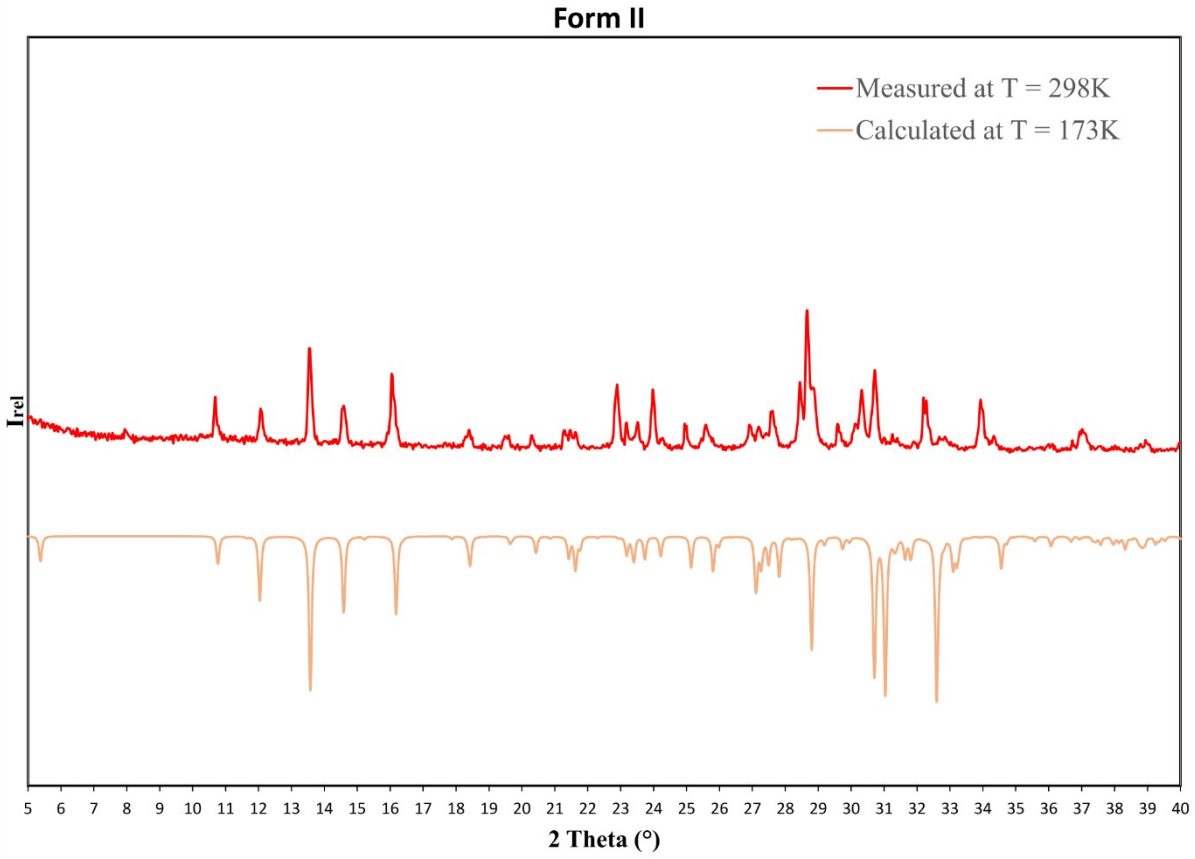

Figure S9. Measured vs. calculated PXRD of the red form **II**.

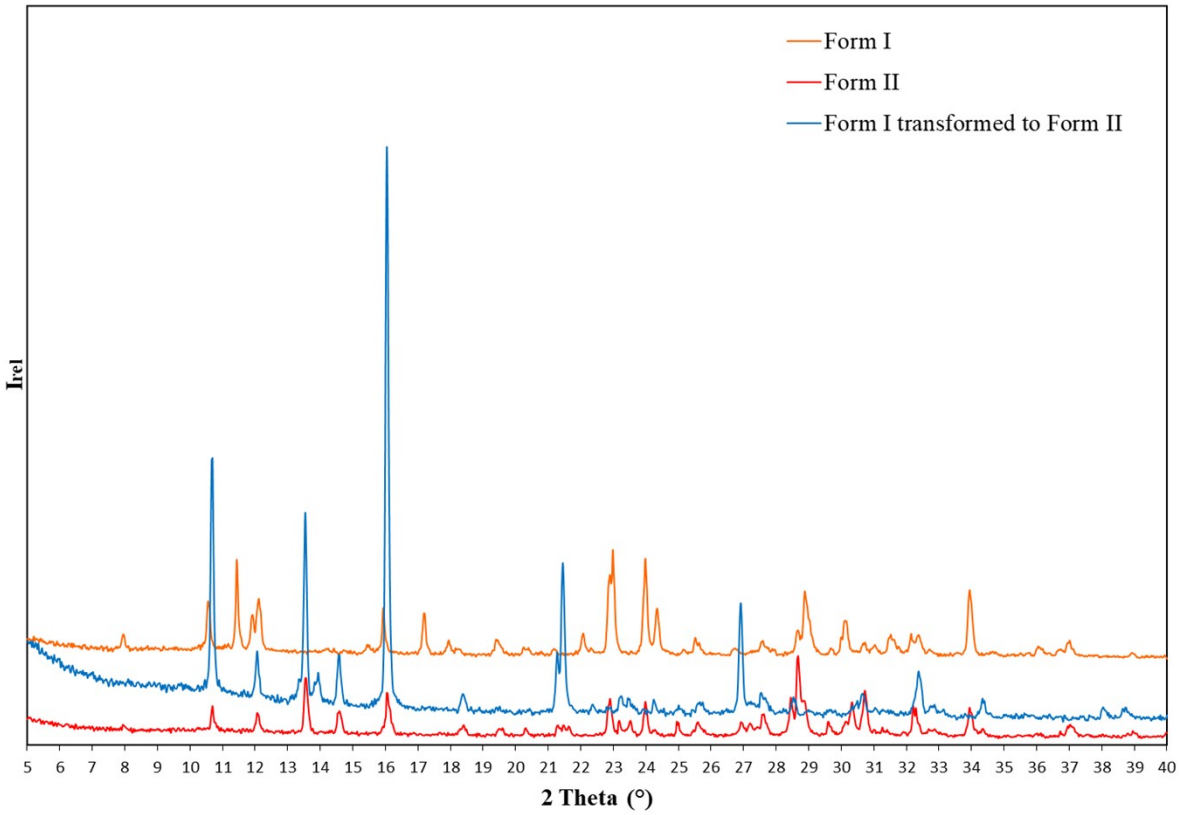

Figure S10. Comparison of the powder x-ray diffraction patterns of forms **I** and **II**, and the powder pattern of a sample of form **I**, heated and transformed to form **II** on the DSC (see description in main article). (Note that peak intensities vary due to preferred orientation.)

H. DSC Results and Traces

Differential scanning calorimetry data (Table S7-9) were collected using a Mettler Toledo 822e with aluminium pans under N_2 gas purge (10 mL/min). *Star SW* 16.20 was used for instrument control and data analysis. Exothermic events were shown as peaks. The temperature and energy calibrations were performed using pure indium (purity 99.99%, m.p. 156.6 °C, heat of fusion 28.45 J g^{-1}) and pure zinc (purity 99.99%, m.p. 419.5 °C, heat of fusion 112 J g^{-1}).

Table S12. Results of DSC traces for **Form I**.

Polymorph at Start	Sample State	Code	Heating Rate / K min^{-1}	T_{onset} / °C	T_{peak} / °C	Integral / J g^{-1}
Form **I**	Crystal	21cm06	10	74.94	80.13	-13.78
Form **I**	Crystal	21cm11	10	73.31	79.80	-13.36
Form **I**	Crystal	21cm12	10	72.23	78.13	-13.71
			Average	**73.49**	**79.35**	**-13.6**
			Standard Deviation	**1.1**	**0.9**	**0.2**

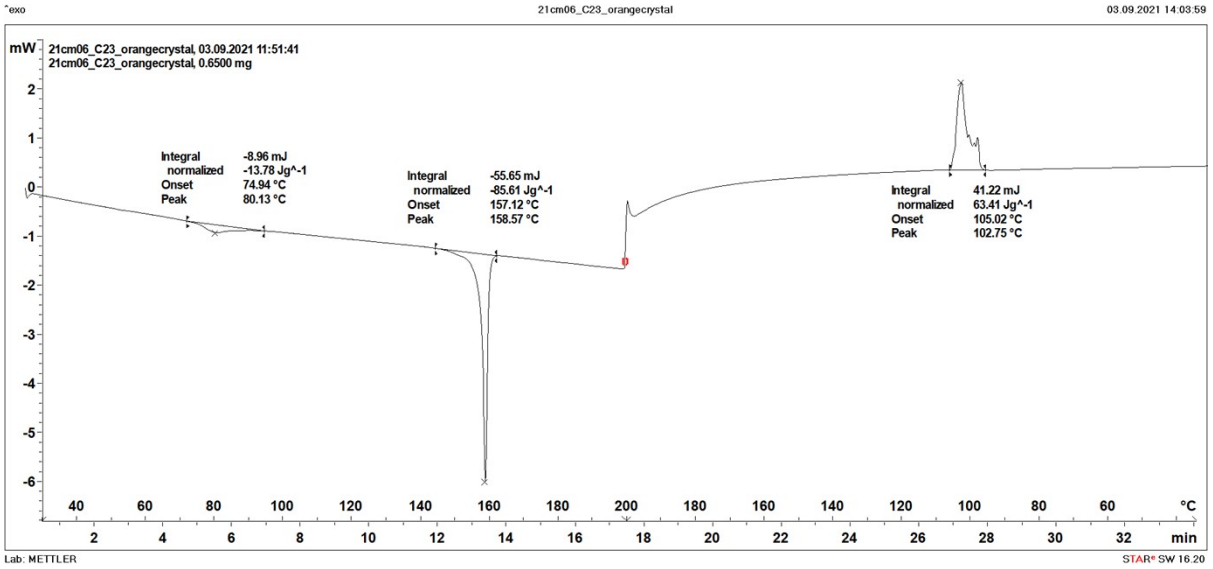
^exo
21cm06_C23_orangecrystal
03.09.2021 14:03:59
mW
21cm06_C23_orangecrystal, 03.09.2021 11:51:41
21cm06_C23_orangecrystal, 0.6500 mg
Integral -8.96 mJ
normalized -13.78 Jg^-1
Onset 74.94 °C
Peak 80.13 °C
Integral -55.65 mJ
normalized -85.61 Jg^-1
Onset 157.12 °C
Peak 158.57 °C
Integral 41.22 mJ
normalized 63.41 Jg^-1
Onset 105.02 °C
Peak 102.75 °C
°C
min
Lab: METTLER
STAR° SW 16.20

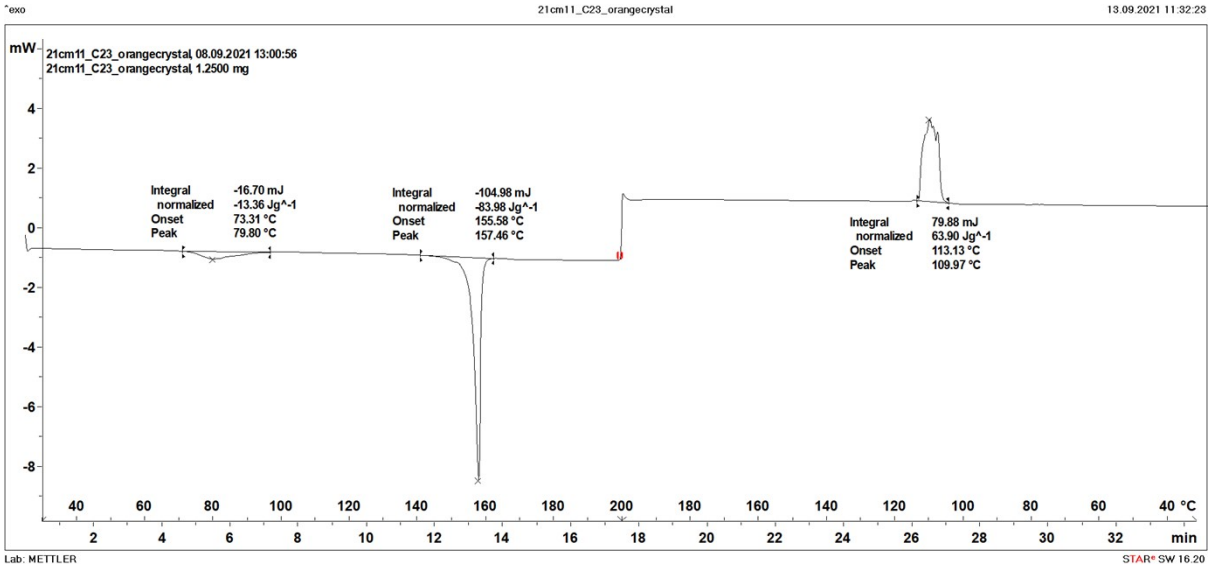
^exo
21cm11_C23_orangecrystal
13.09.2021 11:32:23
mW
21cm11_C23_orangecrystal, 08.09.2021 13:00:56
21cm11_C23_orangecrystal, 1.2500 mg
Integral -16.70 mJ
normalized -13.36 Jg^-1
Onset 73.31 °C
Peak 79.80 °C
Integral -104.98 mJ
normalized -83.98 Jg^-1
Onset 155.58 °C
Peak 157.46 °C
Integral 79.88 mJ
normalized 63.90 Jg^-1
Onset 113.13 °C
Peak 109.97 °C
°C
min
Lab: METTLER
STAR° SW 16.20

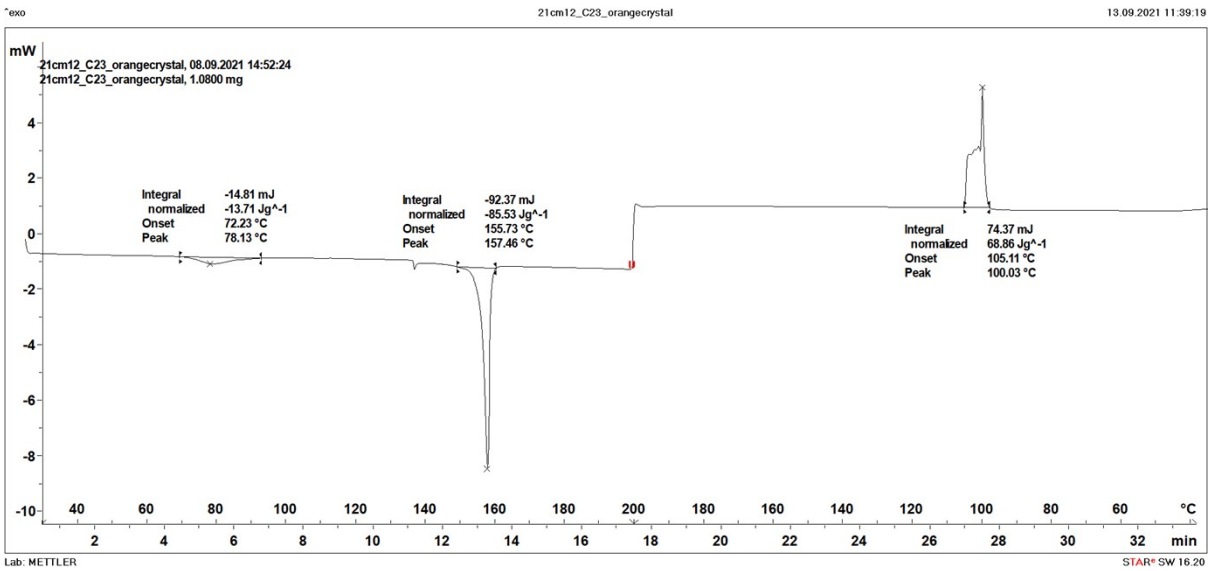
^exo
21cm12_C23_orangecrystal
13.09.2021 11:39:19
mW
21cm12_C23_orangecrystal, 08.09.2021 14:52:24
21cm12_C23_orangecrystal, 1.0800 mg
Integral -14.81 mJ
normalized -13.71 Jg^-1
Onset 72.23 °C
Peak 78.13 °C
Integral -92.37 mJ
normalized -85.53 Jg^-1
Onset 155.73 °C
Peak 157.46 °C
Integral 74.37 mJ
normalized 68.86 Jg^-1
Onset 105.11 °C
Peak 100.03 °C
°C
min
Lab: METTLER
STAR° SW 16.20

Table S13. Results of DSC traces for **Form II**.

Polymorph at Start	Sample State	Code	Heating Rate / K min^{-1}	T_{onset} / °C	T_{peak} / °C	Integral / J g^{-1}
Form **II**	crystal	21as08	10	157.35	159.09	-96.02
Form **II**	ground powder	21cm04	10	157.61	159.46	-98.57
Form **II**	ground powder	21cm05	10	157.60	159.57	-100.50
			Average	**157.5**	**159.4**	**-98.4**
			Standard Deviation	**0.1**	**0.2**	**1.8**

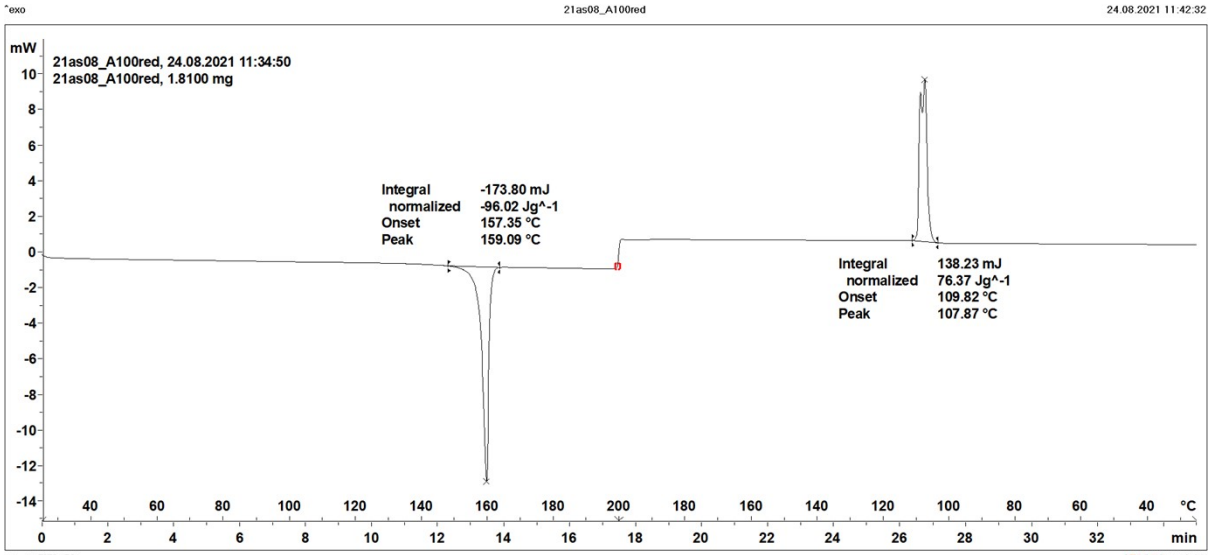
^exo
21as08_A100red
24.08.2021 11:42:32
mW
21as08_A100red, 24.08.2021 11:34:50
21as08_A100red, 1.8100 mg
Integral -173.80 mJ
normalized -96.02 Jg^-1
Onset 157.35 °C
Peak 159.09 °C
Integral 138.23 mJ
normalized 76.37 Jg^-1
Onset 109.82 °C
Peak 107.87 °C
°C
min
Lab: METTLER
STAR° SW 16.20

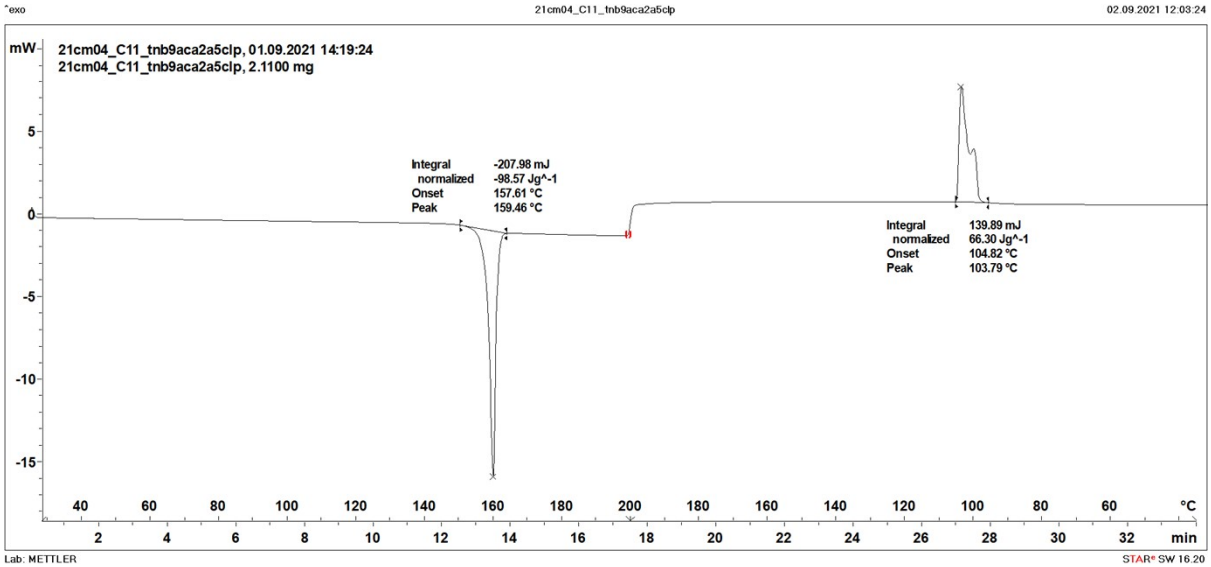
^exo
21cm04_C11_tnb9aca2a5clp
02.09.2021 12:03:24
mW
21cm04_C11_tnb9aca2a5clp, 01.09.2021 14:19:24
21cm04_C11_tnb9aca2a5clp, 2.1100 mg
Integral -207.98 mJ
normalized -98.57 Jg^-1
Onset 157.61 °C
Peak 159.46 °C
Integral 139.89 mJ
normalized 66.30 Jg^-1
Onset 104.82 °C
Peak 103.79 °C
°C
min
Lab: METTLER
STAR° SW 16.20

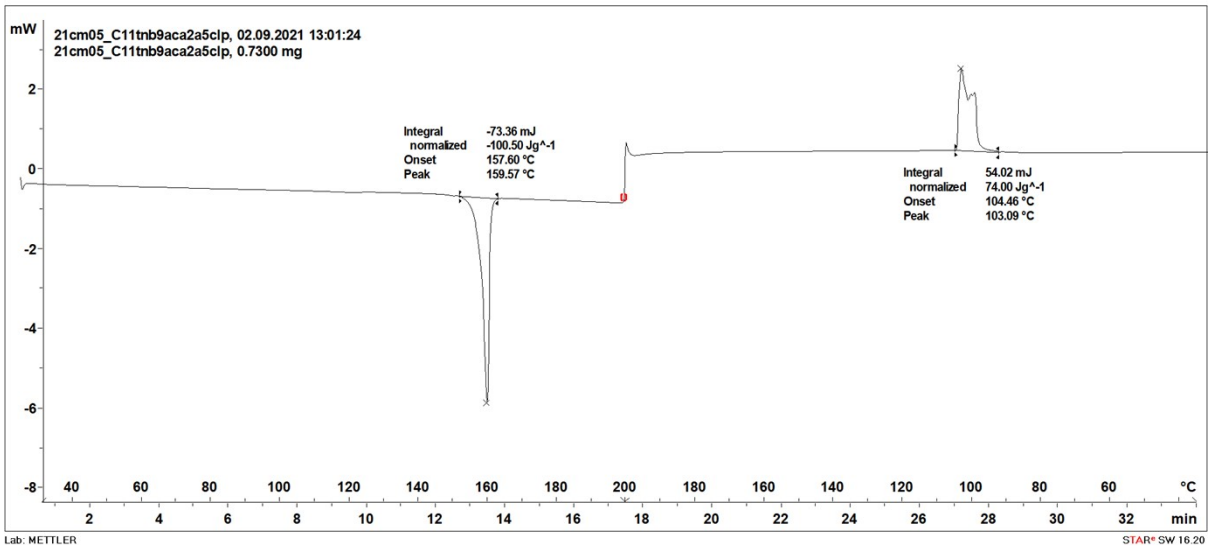
^exo
21cm05_C11tnb9aca2a5clp
02.09.2021 13:29:43
mW
21cm05_C11tnb9aca2a5clp, 02.09.2021 13:01:24
21cm05_C11tnb9aca2a5clp, 0.7300 mg
Integral -73.36 mJ
normalized -100.50 Jg^-1
Onset 157.60 °C
Peak 159.57 °C
Integral 54.02 mJ
normalized 74.00 Jg^-1
Onset 104.46 °C
Peak 103.09 °C
°C
min
Lab: METTLER
STAR° SW 16.20

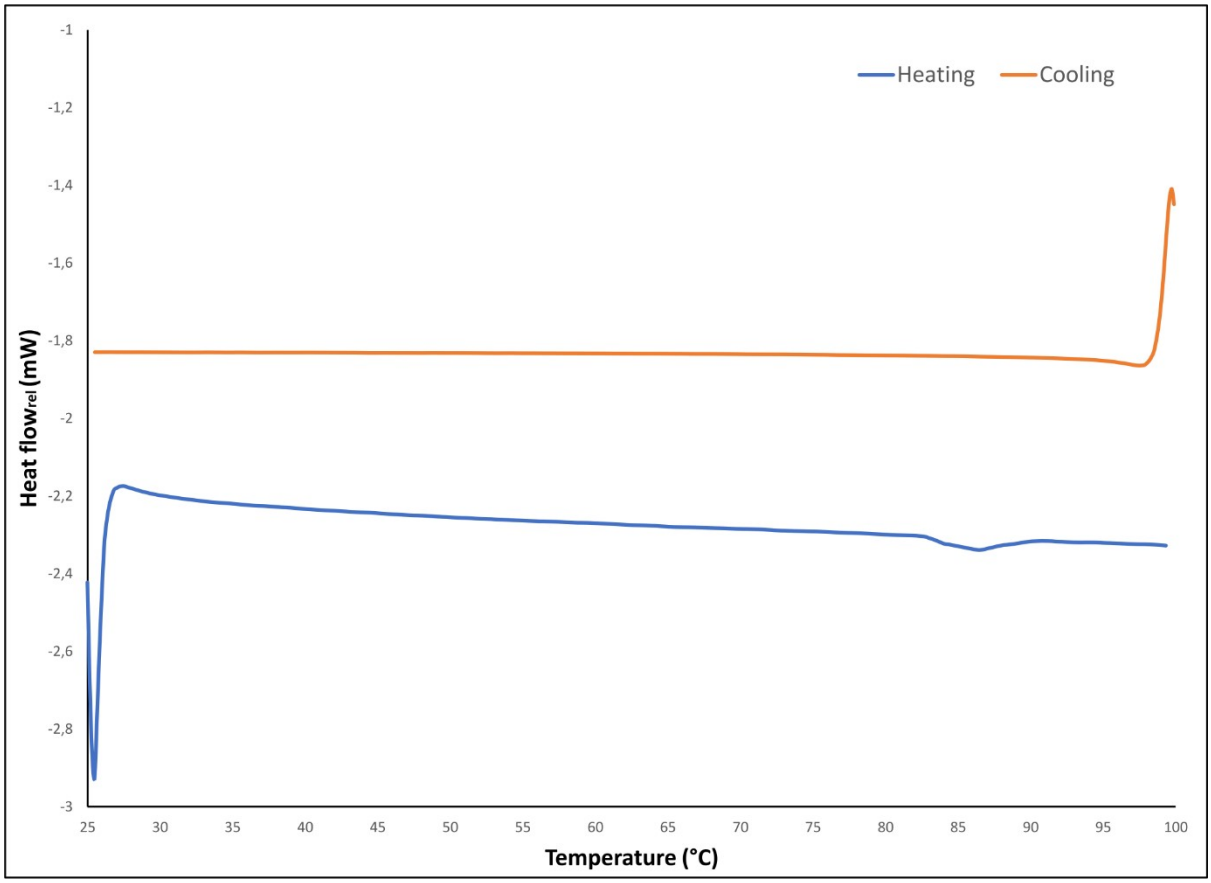

Figure S11. DSC trace of the phase transition of form **I** to form **II**.

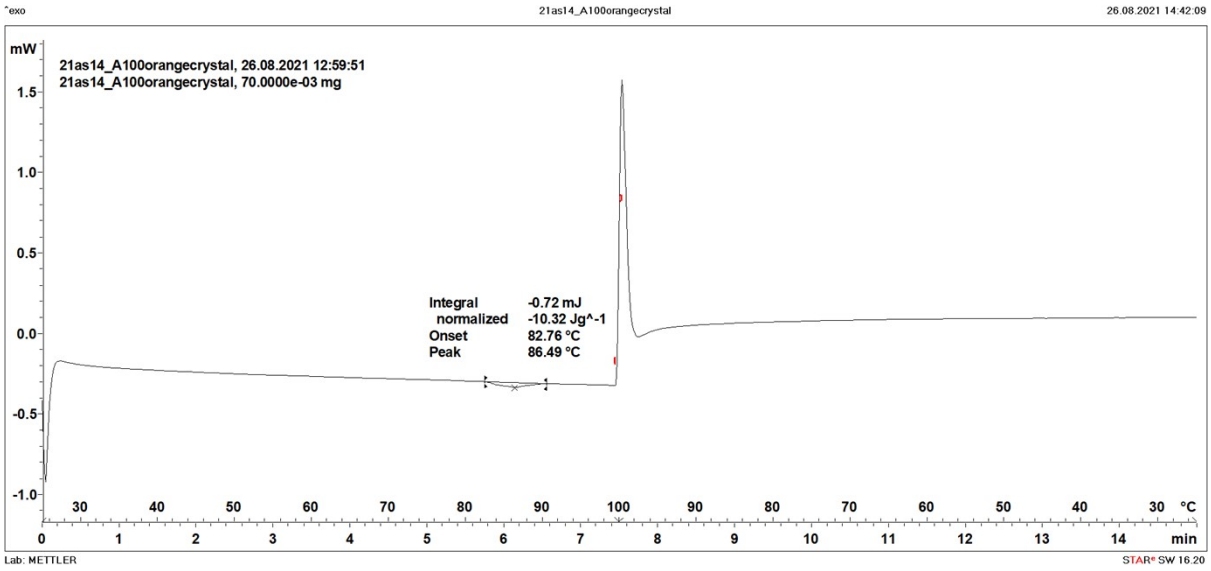

Table S14. Results of DSC traces for slurry experiments.

Experiment Number	Polymorph at Start	Sample State	Code	Heating Rate / K min^{-1}	T_{onset} / °C	T_{peak} / °C	Integral / J g^{-1}
Slurry 1	Form **II**	powder	21as35	10	156.57	158.49	-99.82
Slurry 2	Form **II**	powder	21as36	10	157.88	159.31	-99.12

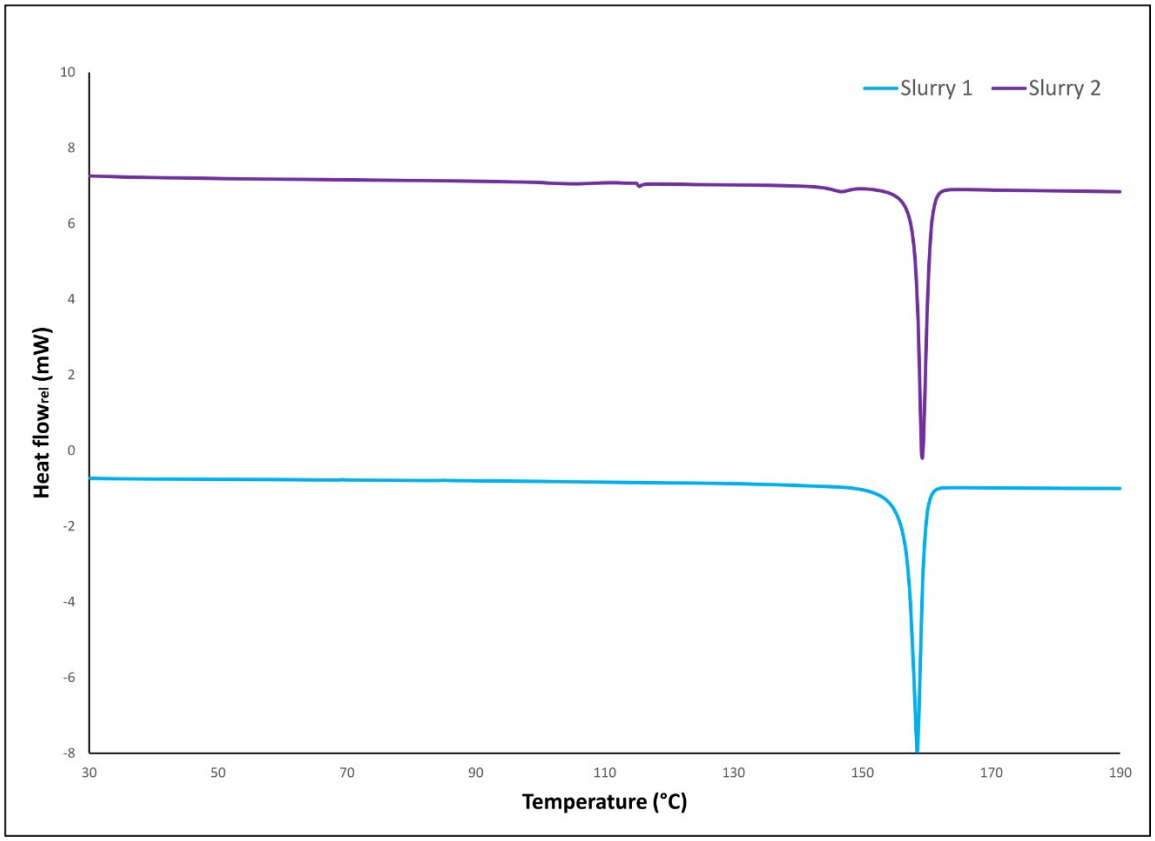

Figure S12. DSC traces of form **II** powders from slurry experiments.

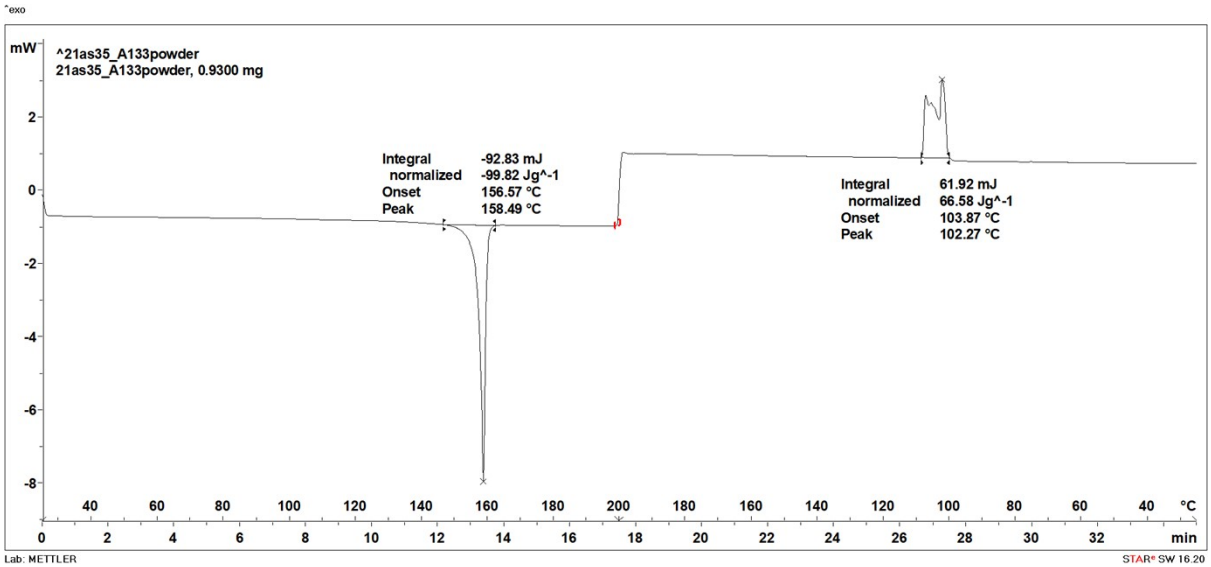
^exo
mW
^21as35_A133powder
21as35_A133powder, 0.9300 mg
Integral -92.83 mJ
normalized -99.82 Jg^-1
Onset 156.57 °C
Peak 158.49 °C
Integral 61.92 mJ
normalized 66.58 Jg^-1
Onset 103.87 °C
Peak 102.27 °C
°C
min
Lab: METTLER
STAR° SW 16.20

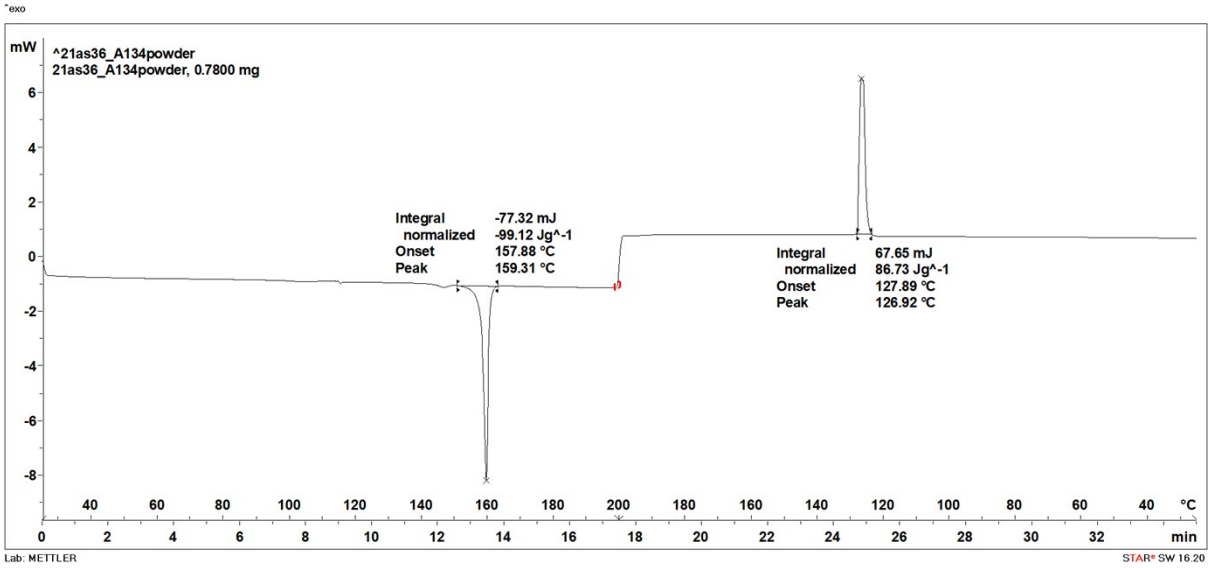
^exo
mW
^21as36_A134powder
21as36_A134powder, 0.7800 mg
Integral -77.32 mJ
normalized -99.12 Jg^-1
Onset 157.88 °C
Peak 159.31 °C
Integral 67.65 mJ
normalized 86.73 Jg^-1
Onset 127.89 °C
Peak 126.92 °C
°C
min
Lab: METTLER
STAR° SW 16.20

I. Variable Temperature Single Crystal X-ray Diffraction

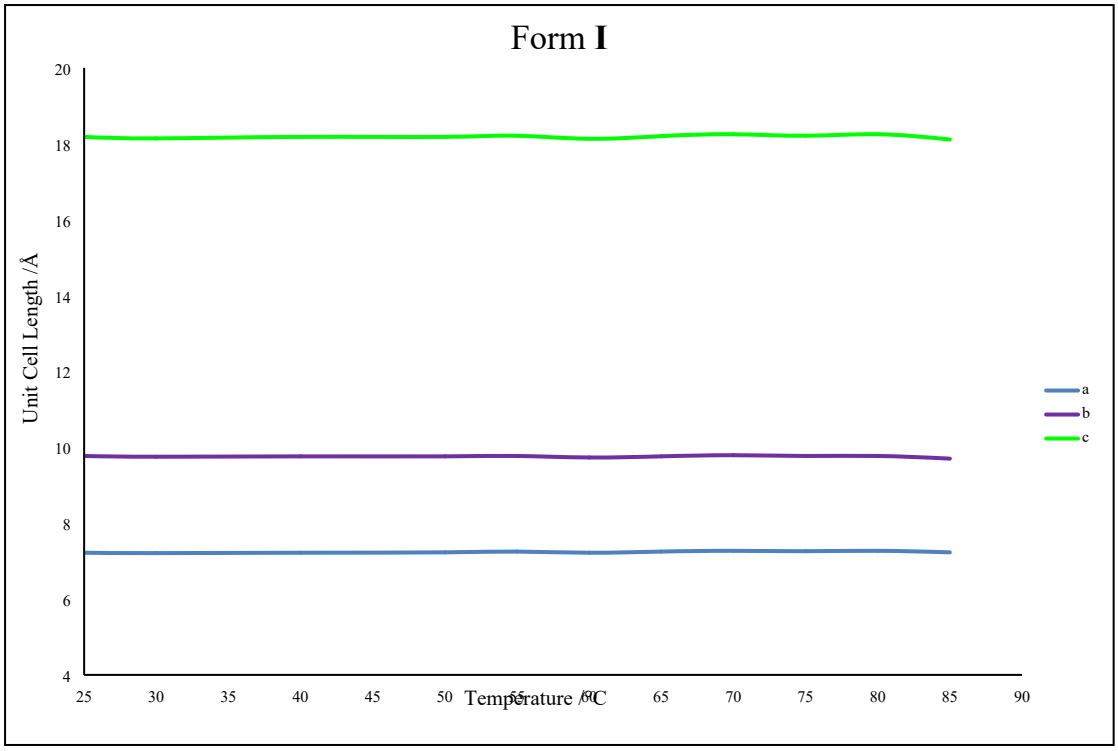

Figure S13. Variable temperature SCXRD determination of unit cell lengths of form **I** with an increase in temperature.

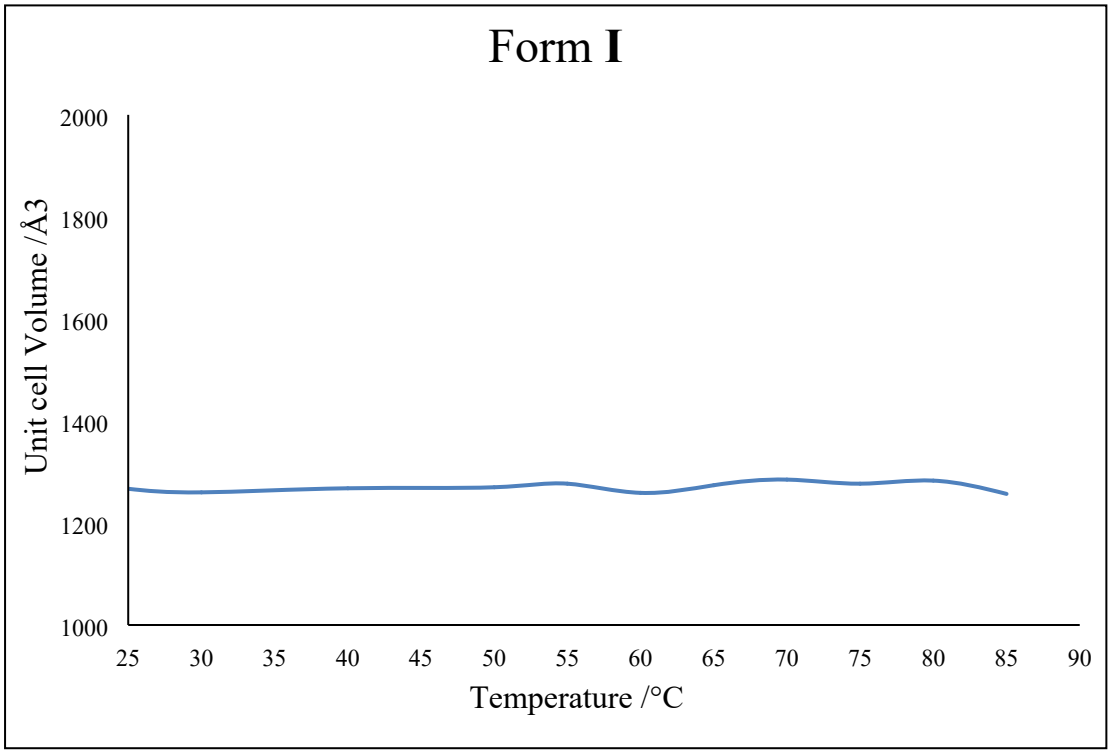

Figure S14. Variable temperature SCXRD determination of cell volume of form **I** with an increase in temperature.

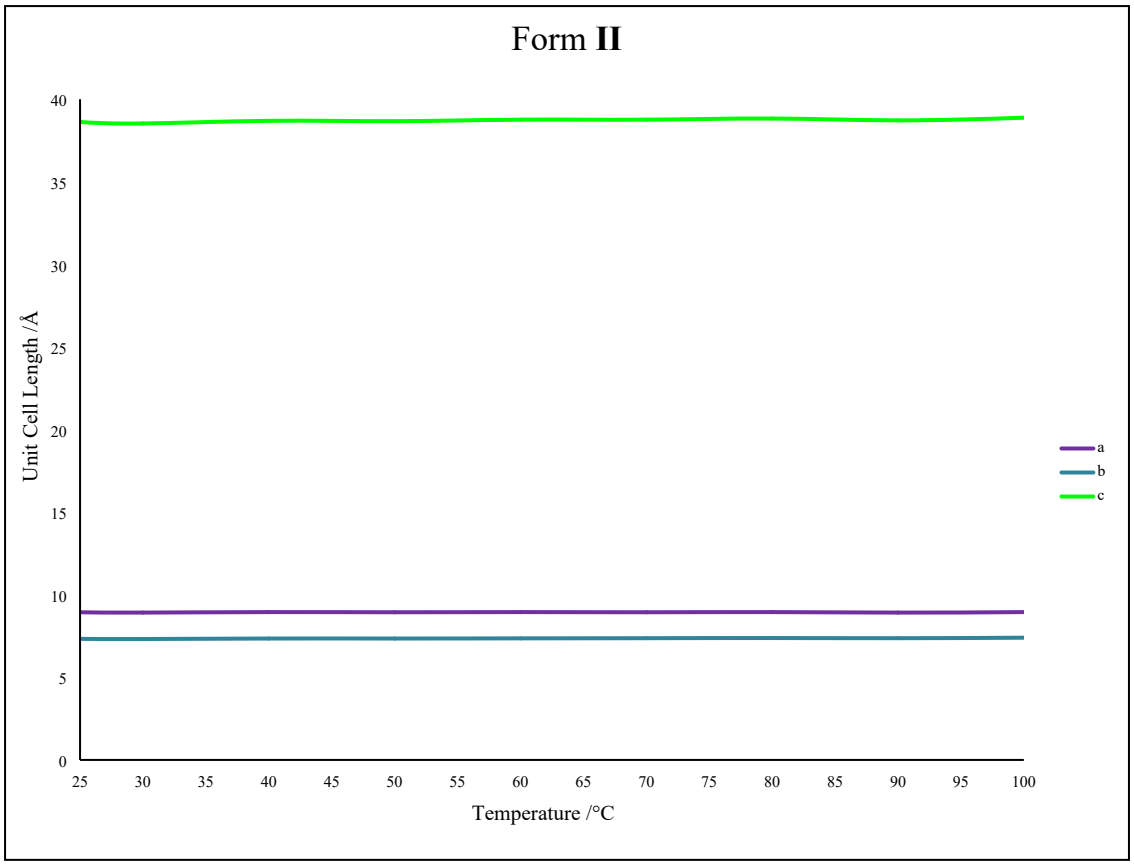

Figure S15. Variable temperature SCXRD determination of unit cell lengths of form **II** with an increase in temperature.

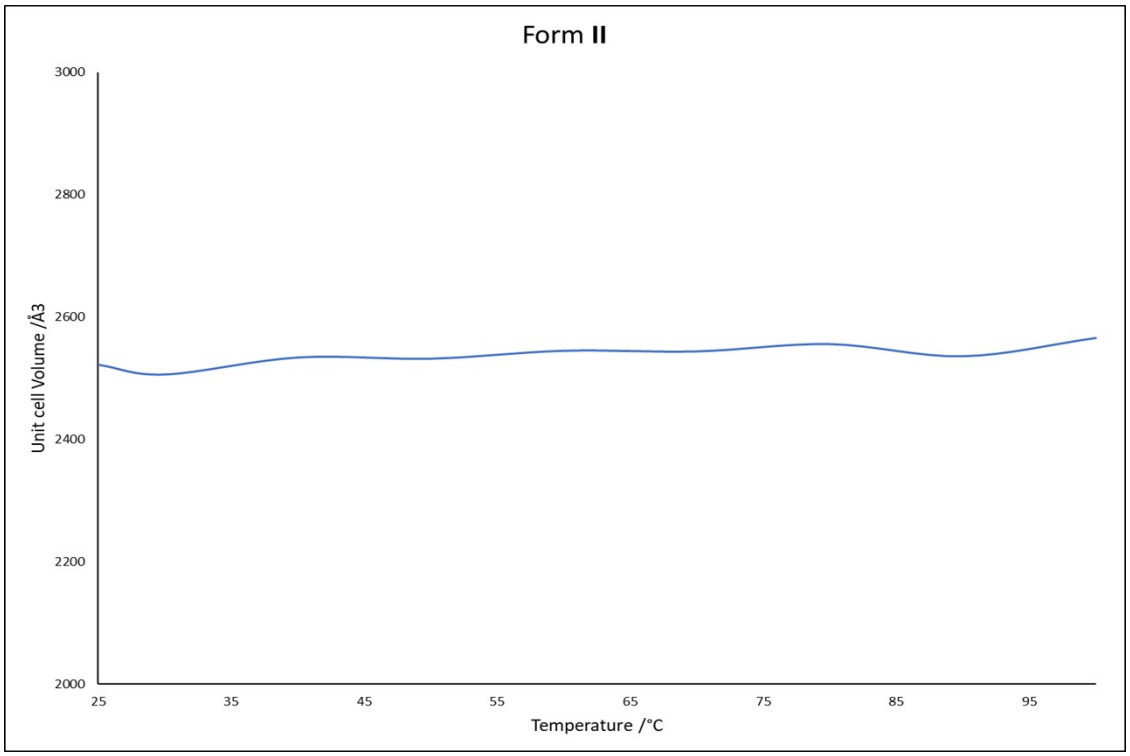

Figure S16. Variable temperature SCXRD determination of cell volume of form **II** with an increase in temperature.

J. Photoluminescence Spectroscopy

Photoluminescence spectra of samples of form **I** and form **II** were acquired at room temperature using a Horiba QuantaMaster 8000 spectrofluorometer with a Xe lamp and a Hamamatsu R2658 PMT detector. The excitation wavelength used was 469 nm. This value was determined via a PLE spectrum to be the wavelength that gave a maximum emission intensity at 650 nm for Form I. The PL spectra are both emission corrected for the throughput of the emission monochromator and the detector efficiency.

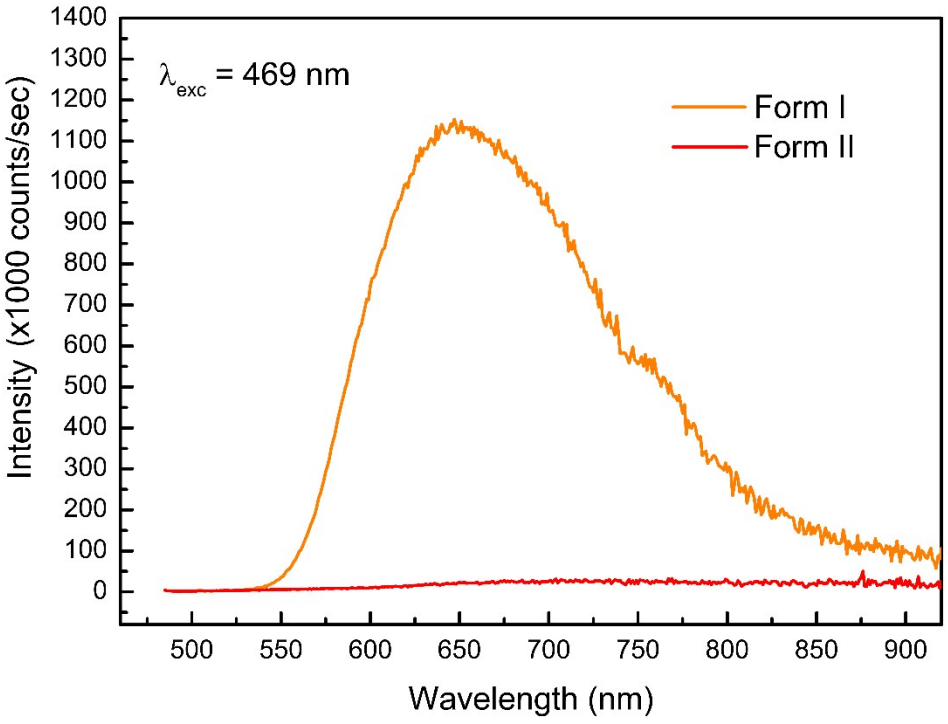

Figure S17. Photoluminescence spectra of form **I** and form **II** acquired under exactly the same measurement conditions.

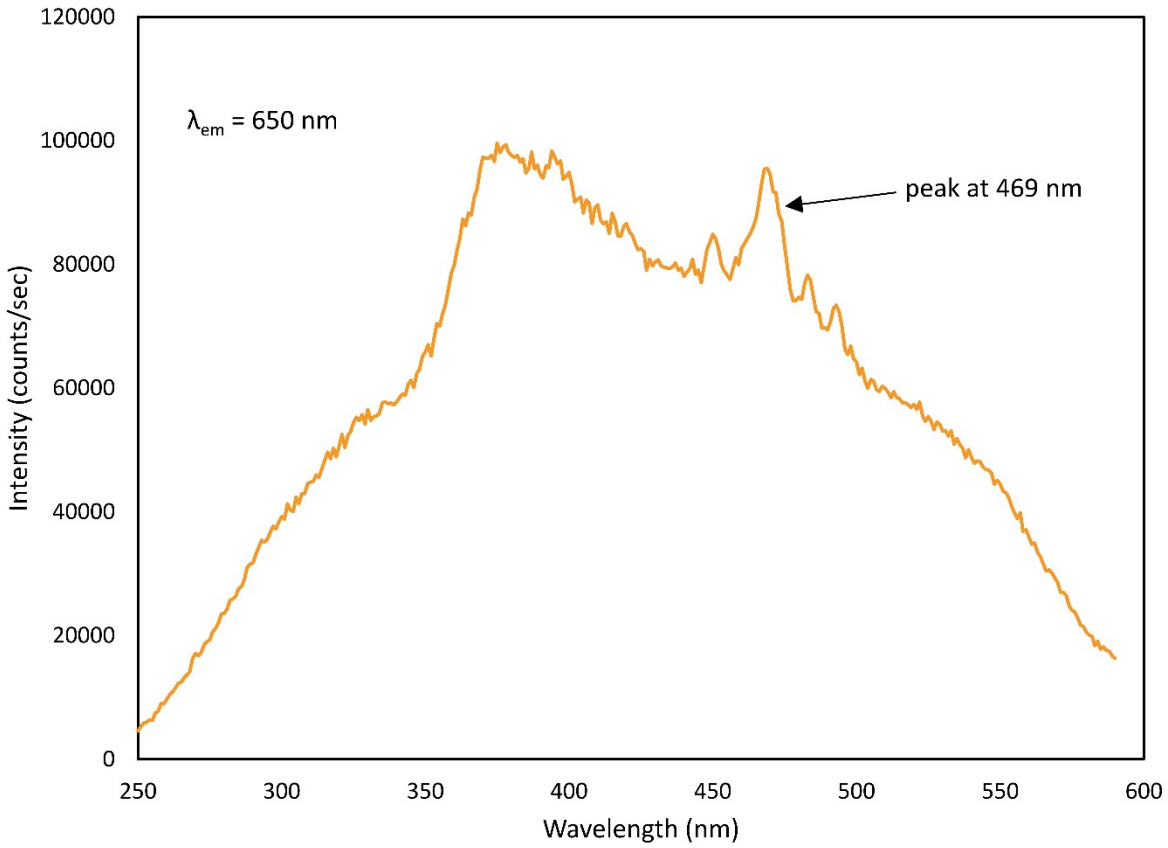

Figure S18. The figure shows the photoluminescence excitation spectrum for Form **I**, where emission at 650 nm was monitored. The peak at 469 nm is indicated and is the justification for our choice of 469 nm as the excitation wavelength for the steady-state PL emission spectra

K. Nuclear Magnetic Resonance Spectroscopy

1H NMR spectra were recorded on a Bruker Avance III (500 MHz) spectrometer. An NMR sample of tnb, 9aca, and 2a5clp (combined in a 1:1:1 stoichiometric ratio) was prepared in acetone. Chemical shifts are reported in parts per million (ppm) relative to the tetramethylsilane (TMS) referenced against the protonated solvent (acetone). Coupling constants (*J*) are reported in Hertz (Hz). Reported NMR splitting signals are abbreviated as follows: s = singlet, d = doublet, and t = triplet.

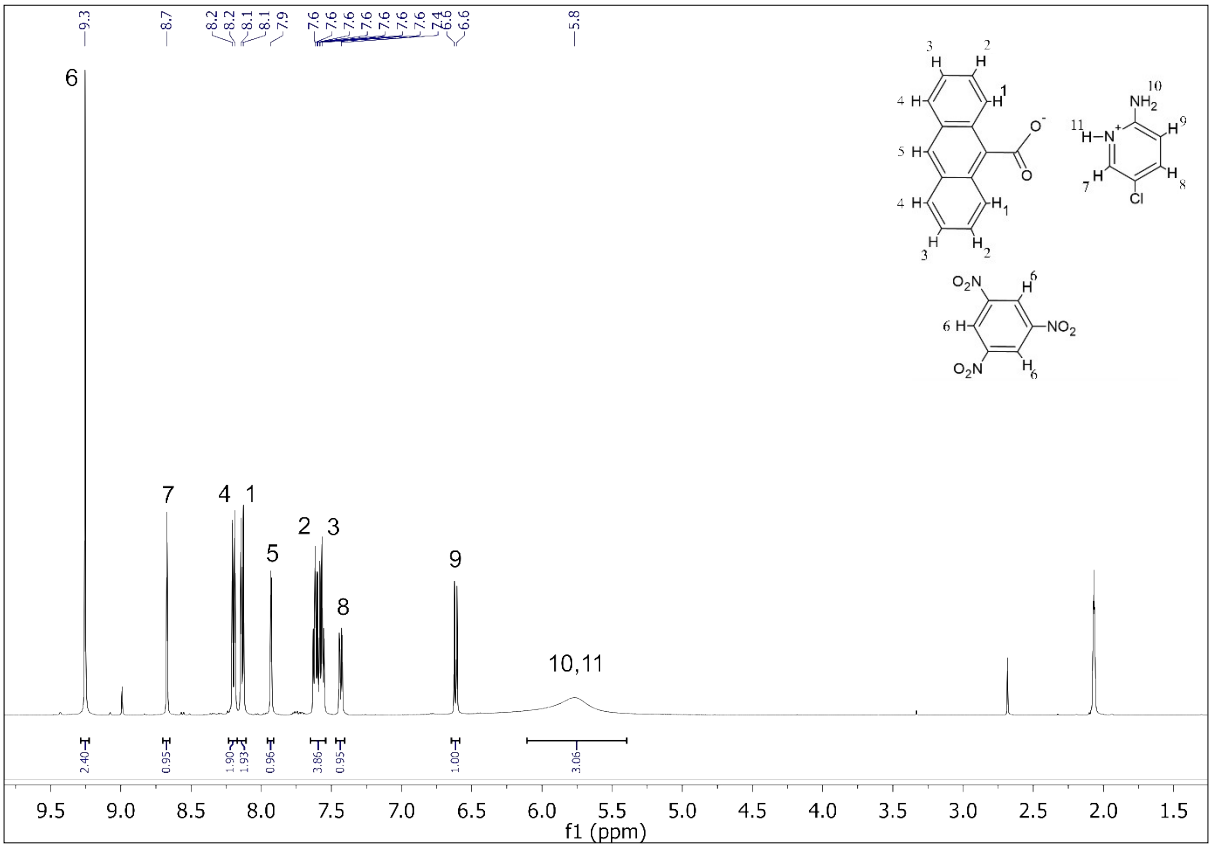

Figure S19. [1]H NMR spectrum of tnb+9aca+2a5clp in acetone.

Table S15. NMR peak assignments.

Peak position (ppm)	Integration	Multiplicity	Assignment
9.3	3H	s	6
8.7	1H	s	7
8.2	2H	d	4
8.1	2H	d	1
7.9	1H	s	5
7.6	2H	t	2
7.6	2H	t	3
7.4	1H	d	8
6.6	1H	d	9
5.8	3H	s	10 and 11